Simulation of Density Flow in Dam Reservoirs Using Two Dimensional Mathematical Models

Fatih Üneş[1], Necati Ağiralioğlu [2], Mustafa Demirci[3]

[1,3,] *Department of Civil Engineering, Mustafa Kemal University, İskenderun, Hatay-Turkey*

[2]*İstanbul Technical University, Civil Engineering Faculty,, Maslak, İstanbul - Turkey.*

ABSTRACT

Density inflow is modeled in two dimensions through a reservoir with sloping bottom. If an inflow of higher density enters ambient dam reservoir water, then it plunges below the ambient water and then becomes density underflow. In the present model, nonlinear and unsteady continuity, momentum, energy and turbulence model equations are formulated in the Cartesian coordinates. For the turbulence viscosity, k-ε turbulence model is used with an extension to include production or destruction of turbulent kinetic energy. In order to investigate the Coriolis force effect on the density flow in a dam reservoir, Coriolis force parameter is included in the governing equations. The equations of the model are solved based on the initial and boundary conditions of the dam reservoir flow for a range of bottom slopes. The results of the present model are compared with the previous experimental work and the mathematical model. Present model results are found to be of the same magnitude as the experimental measurements

Keywords: Dam, reservoir, underflow, mathematical model, simulation.

INTRODUCTION

Inflow river water polluted from industrial plants, household and also power stations may have different temperatures, concentration of dissolved or suspended substances from the ambient water in a dam reservoir. The ambient water has seldom the same density difference with inflow river water. The differences lead to baroclinic forces affecting the flow structure. If such inflow river water enters ambient dam reservoir water, then three basic types of currents may occur. These are called the over flow; inter flow, and plunging flow [1-2]. If density of incoming flow is smaller than ambient water body in the reservoir, this type of flow will move along the free surface and is called over flow. If reservoir ambient water is stratified due to temperature or other effects, incoming flow will go forward an intermediate layer that density of this layer is equal to inflow density. This flow is called inter flow. However, if a river water flowing density is denser than quiescent water density of dam reservoir, then this type of flow will plunge below the ambient water and will move along the reservoir bottom. This flow is named underflow, density negatively buoyant flow or plunging flow and is the subject investigated in this study in a three-dimensional reservoir with a sloping bottoms and divergence angles.

The definition sketch of plunging flow and initial entrainment coefficient are shown in Fig. 1 [3-4]. This figure shows a plunging flow situation in a sloping bottom two-dimensional

reservoir. In Figure 2, H_p, is plunge depth, H_d, is the depth of the underflow layer, U_d is underflow layer mean velocity, q_d is underflow layer stream discharge along the density flow and U_{in} is river inflow mean velocity.

In this type of flow, the river inflow plunges at a place on ambient reservoir water surface that is known as plunge point or plunge line.

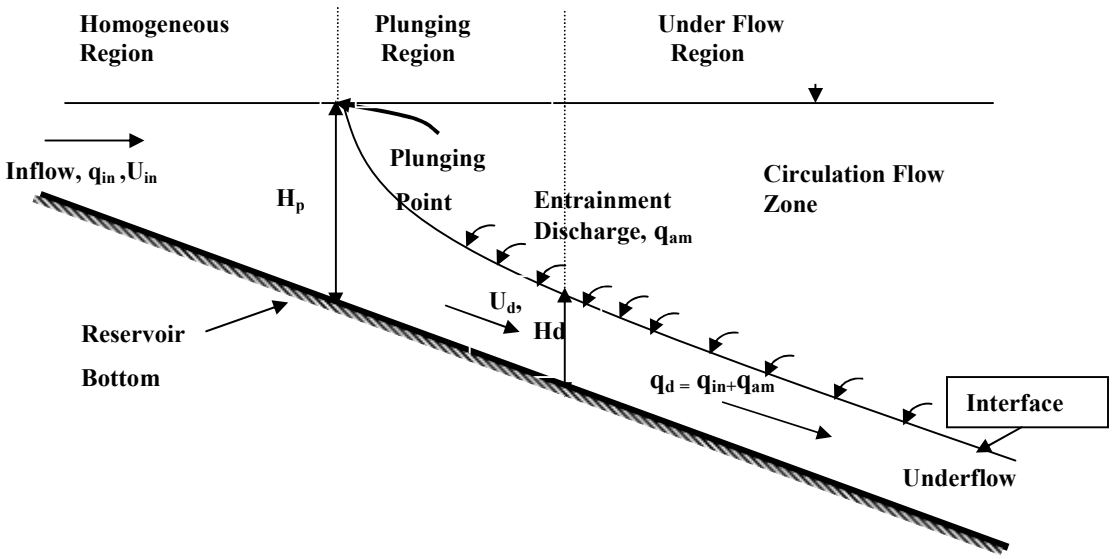

Figure 1 Sketch of plunging flow and development of mixing rate

Density flow is studied herein in a two dimensional reservoir with a sloping bottom. Laboratory experimental studies of density plunging flows over both sloping bottom and diverging horizontal channel were performed by a lot of researchers that most of them established a number of semi empirical equations [5-10]. A few authors have considered the problem by solving it using numerical methods [1- 4, 7 and 11]. They established mathematical models and used numerical solution to investigate the plunging and underflow.

In the numerical approach, plunge region need not be isolated from the rest of the reservoir so that the river inflow can be simulated along the reservoir. In this solution, plunge region will appear in the emerging flow field as a part of the overall solution. Such a solution gives realistic and useful results.

PRESENT STUDY

In this paper, solutions were obtained for flows corresponding to both the experimental runs of Singh and Shah [5] and the mathematical model of Farrell and Stefan [3]. Singh and Shah experimental runs applied turbulence flow conditions where Reynolds numbers are taken as 600-11000. Farrell and Stefan model is based on Singh and Shah experimental runs using cylindrical coordinates in two-dimensional reservoir.

Inflow to shallow dam reservoir may be in virtually constant depth and strongly diverging channel. Inflow to a reservoir in a narrow walley may have little divergence and more slope effect [7]. So apart from reservoir geometry, various extraneous forces or factors such as wind, waves etc. can exert an influence on the plunging flow dynamics. These forces, in particularly, can be expected to move the plunge point on the water surface. If density differences are due to dissolved or suspended materials, then buoyancy flux may change and

influence the plunging flow dynamics. Some of the above mentioned factors are omitted in the present model in order to facilitate the solution, even though, they may have some effects over the reservoir flow.

Since this work is limited to 2-D, the width of the reservoir is not considered, meaning the divergence of the reservoir is not studied. The temperature effects caused by meteorological inputs are not considered in this study.

Based on the initial and boundary conditions of the reservoir flow, equations presented later in this article are solved using control volume concept with computational fluid dynamic solver Fluent 5.3 software program. In these model simulations, it is assumed that density flows occur only due to differences in temperatures of ambient water and inflow water.

MATHEMATICAL MODEL EQUATIONS

The reservoir configuration is accommodated in two dimensional (x,y) Cartesian coordinates. The experimental reservoir configuration of Singh and Shah [5] is used in the present paper as well as in Farrell and Stefan [3] mathematical model simulation. In this density different reservoir, flows such as stratified, plunging and circulation can occur and these types of flows are very complicated and hard to solve. Therefore, some simplification process has to be made before presenting the governing equations.

Because the free surface phenomena such as wind or wave effects are not being considered in reservoir surface, the free surface of the reservoir is modeled as a rigid lid during the present model simulation. Another simplification is that the temperature difference is taken to be the source of the stratified and buoyancy flows [4, 12]. From field and practice, small temperature differences are enough to produce density flow in the reservoir [3].

Therefore, the density-temperature relation can be linearized and written as follows:

$$\Delta\rho = \rho - \rho_0 = \beta\rho_0\left[T_0 - T\right] \tag{1}$$

where ρ is the water density, T is the water temperature and β is the coefficient of thermal expansion and is calculated as $\beta = -(\Delta\rho/\rho_o)(1/\Delta T)$, where ΔT is the temperature difference between ambient and inflow river waters, ρ_o and T_o refer to the reservoir conditions. Equation (1) will be substituted into the momentum equation. In the present mathematical model application of the Boussinesq approximation and reduced pressure approach is considered as another simplification.

The mathematical model consists of the following equations: the continuity equation, momentum equations, energy equation and the turbulence model equations.

Continuity equation

$$\frac{\partial\rho}{\partial t} + \frac{\partial(\rho\bar{u})}{\partial x} + \frac{\partial(\rho\bar{v})}{\partial y} = 0 \tag{2}$$

Momentum equations

For the x axis,

$$\frac{\partial\bar{u}}{\partial t} + \bar{u}\frac{\partial\bar{u}}{\partial x} + \bar{v}\frac{\partial\bar{u}}{\partial y} - f\bar{v} = \frac{1}{\rho}\frac{\partial\bar{P}}{\partial x} + \frac{\partial}{\partial x}\left(\nu_{eff}\frac{\partial\bar{u}}{\partial y} + \frac{\partial\bar{v}}{\partial x}\right) + g \tag{3}$$

and for the y axis,

$$\frac{\partial \bar{v}}{\partial t} + \bar{u}\frac{\partial \bar{v}}{\partial x} + \bar{v}\frac{\partial \bar{v}}{\partial y} = \frac{1}{\rho}\frac{\partial \bar{P}}{\partial x} + \frac{\partial}{\partial y}\left(\nu_{eff}\frac{\partial \bar{u}}{\partial y} + \frac{\partial \bar{v}}{\partial x}\right) + g\beta(T_o - \bar{T}) \tag{4}$$

Energy equation for the temperature.

$$\frac{\partial \bar{T}}{\partial t} + \bar{u}\frac{\partial \bar{T}}{\partial x} + \bar{v}\frac{\partial \bar{T}}{\partial y} - f\bar{u} = \alpha_{eff}\left(\frac{\partial^2 \bar{T}}{\partial x^2} + \frac{\partial^2 \bar{T}}{\partial y^2}\right) \tag{5}$$

where $\bar{u}$ and $\bar{v}$ are the mean velocities in the x and y directions, respectively, ρ is the water density, $\bar{P}$ is the pressure adjusted to absorb the hydrostatic portion of the gravity terms and $\bar{T}$ is the mean temperature, $\nu_{eff} = \nu + \nu_t$, where ν is the kinematic viscosity and ν_t is the kinematic eddy (turbulence) viscosity; and $\alpha_{eff} = (\nu / Pr) + (\nu_t / \sigma_t)$ where Pr and σ_t are the Prandtl and turbulent Prandtl numbers, respectively.

k-ε turbulence model equations

The effect of turbulence is simulated using the modified standard k-ε model including the suitable buoyancy terms. Standard k-ε model is semi–emprical model Launder and Spalding [13-14] based on model transport equations for turbulent kinetic energy (k) and its dissipation rate (ε). In the derivation of the k- ε model, it was assumed that the flow is fully turbulent, and the effects of molecular viscosity are negligible. The standard k-ε model is therefore valid only for fully turbulent flows. k-ε transport equations has been implemented by Rodi [15]. For a two dimensional unsteady flow at the sloping bottom reservoir, the eddy viscosity ν_t is computed from the following equation,

$$\nu_t = C_\mu \frac{k^2}{\varepsilon} \tag{6}$$

where k is the turbulent kinetic energy and ε is the turbulent energy dissipation rate per unit mass. k and ε are obtained from the solution of the following equations in two-dimensional flow [3].

Equation of k

$$\frac{\partial k}{\partial t} + \bar{u}_j\frac{\partial k}{\partial x_J} = \frac{\partial}{\partial x_j}\left[\left(\nu + \frac{\nu_t}{\sigma_k}\right)\frac{\partial k}{\partial x_J}\right] + Prod + G - \varepsilon \tag{7}$$

and equation of ε,

$$\rho\frac{\partial \varepsilon}{\partial t} + \bar{u}_j\frac{\partial \varepsilon}{\partial x_J} = \frac{\partial}{\partial x_j}\left[\left(\nu + \frac{\nu_t}{\sigma_\varepsilon}\right)\frac{\partial \varepsilon}{\partial x_J}\right] + C_{1\varepsilon}\frac{\varepsilon}{k}Prod - C_{2\varepsilon}\frac{\varepsilon^2}{k} + C_{1\varepsilon}C_3\frac{\varepsilon}{k}G \tag{8}$$

where Prod is the production of turbulent kinetic energy from the mean flow and is given as

$$Prod = \nu_t\left(\frac{\partial \bar{u}_i}{\partial x_j} + \frac{\partial \bar{u}_j}{\partial x_i}\right)\frac{\partial \bar{u}_i}{\partial x_j} \tag{9}$$

In these equations, G is the production or destruction of turbulent kinetic energy by buoyancy forces and is given as

$$G = g_i\beta\frac{\nu_t}{\sigma_t}\frac{\partial \bar{T}}{\partial x_i} \tag{10}$$

The values of the coefficients C_μ, $C_{1\varepsilon}$, $C_{2\varepsilon}$, C_3, σ_k, σ_k, and σ_t appearing in the k-ε turbulence model equations used herein were given the standard values recommended by Launder and

Spalding (1974). For the standard k-ε model, these constants are taken as $C_\mu = 0.09$, $C_{1\varepsilon} = 1.44$, $C_{2\varepsilon} = 1.92$, $\sigma_k = 1.00$, $\sigma_k = 1.3$, and $\sigma_t = 0.9$. C_3 is not part of the standard k-ε model but enter through the buoyancy terms and the constant C_3 is not stable value. In FLUENT, C_3 is not specified, but is instead calculated according to $C_3=\tanh|v/u|$, where v is the component of the flow velocity parallel to the gravitational vector and u is the component of the flow velocity perpendicular to the gravitational vector (FLUENT, [16]).

Boundary and Initial Conditions

Since reservoir density flow is unsteady, turbulence flow field boundary conditions must be specified individually on the reservoir inlet and outlet planes, at the walls and at the free surface. Boundary and initial conditions for each variable are chosen individually.

Velocity is given a symmetry condition at the free surface. At the reservoir bottom and dam face, velocities are determined using the standard wall function that is based on the proposal of Launder and Spalding [14]. This function assumes a log-law velocity profile near the wall and is provided in FLUENT as follows.

$$\frac{u_p}{u_*} = \frac{1}{K}\ln\left(E\frac{u_* y_p}{v}\right) - \Delta B \tag{11}$$

where, u_p is the mean flow velocity at point p; u_* is the friction velocity; K is the von Karman constant; E is the empirical constant having a value of 9.81; y_p is the distance from point p to the wall; and ΔB is the roughness function that depends, in general, on the wall roughness height, Ks. At the inflow boundary, the horizontal velocity component in the x direction, u, is given uniform velocity distribution. The vertical velocity component in the y direction, v, is set to zero. At the outflow point of the reservoir, the horizontal velocity component is allocated a value in order to exactly balance inflow and the vertical velocity component is taken as zero. The initial velocity field into the reservoir consists of a forward horizontal velocity, u, and zero vertical velocity, v, at all points except close to dam.

The bottom and the free surface of the reservoir's temperatures are taken as adiabatic. The initial temperature field consists of a constant temperature throughout the reservoir. The dam face temperature is taken equal to the initial temperature of the reservoir water. The inflow river water temperature is set at a constant value with no variation over river depth. Reservoir temperature conditions will be changed later during the simulation run time.

MODEL APLICATION

In order to examine plunging flow models, model solutions were extracted for flows corresponding to the experimental runs of Singh and Shah [5]. and Farrell and Stefan [3]. Their experimental reservoir configuration was taken from their paper and the project report. The reservoir shape is shown schematically in Fig. 2.

Experimental and model reservoir flows were simulated in a reservoir 12.5 m long where the reservoir inlet and outlet average depths are changed between 3.5 - 16 cm and 16 - 41 cm, respectively. The computational domains are divided into 125x17 grids in the *x* and *y* directions, respectively and 2125 cells. As an initial condition, the inflow channel is first filled with warm water, and then the cold water is released at the upstream end of the inflow channel at a specified rate. The current proceeds forward until it reaches the downstream boundary. The inlet densimetric Froude number in all cases exceeds unity, indicating an

incoming supercritical flow condition. The calculation continued for approximately 800 s at which point the front has long past the downstream boundary and any change in the flow field would be insignificant. In order to have the desired converged solution, a time step of 10 seconds was chosen after preliminary trials.

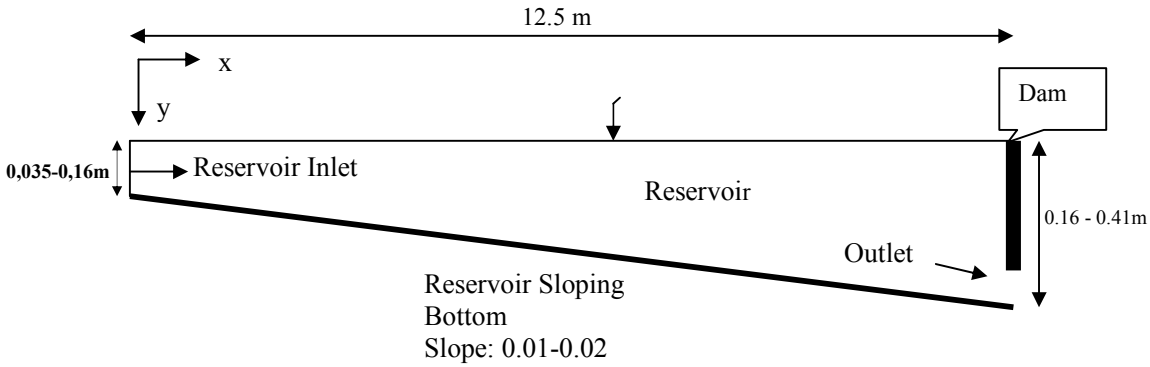

Figure 2. Schematic projection of model simulation for sloping reservoir

ANALYSIS OF THE RESULTS

In the present mathematical model, a number of flows were simulated within the variable ranges given with the experimental runs of Singh and Shah [5]. Farrell and Stefan [3] used the same variable ranges in their mathematical model simulation. The present model simulations were carried out for a range of flow conditions. These simulations yielded realistic plunging flow fields in all runs and were developed in a similar manner as described by Singh and Shah (1971). The details of these runs are given in Table.1.

Table.1 Details of reservoir plunging flow simulations for the present model

Run No:	Bottom Slope	Inflow Channel Depth (cm)	Inflow Velocity (cm/s)	Inflow Stream Discharge ($cm^3/cm/s$)	Ambient Water Temp. T_o (^0C)	Inflow Water Temp. T_{in} (^0C)	Plunge Depth by Farrell and Stefan (1986) (cm)	(Present Model) After Plunge First Appearing	
								Plunge Depth H_p (cm)	Distance from Inlet X (m)
SSHAH 3	0.0104	8.3	3.71	30.8	25	15	12.4	12.7	4.3

Temporal variation of velocity field

The velocity field in the present paper is developed in a similar manner as both the available experimental and mathematical model simulation results. In all run simulations, initially the inflow river water (cold water) advanced into the reservoir, pushed forward under the ambient

warm water and then the warm water is displaced forward and the velocities are in the downstream direction at all points. The warm water is initially displaced forward and velocities are forward at all points. When the denser cold water pushed slightly forward under the warm water, consequently a small region of (back) recirculation flow appeared in the ambient water surface. In this way plunging flow started and then the river inflow cold-water flow downstream under the ambient warm water as a density current. This backflow region grew larger as time elapsed and then eventually the density current front reached the dam base and the entire ambient warm water zone is transformed into a recirculation zone and a stratified flow is produced along the reservoir. Plunge point was well defined in these simulation velocity fields.

Typical velocity fields for the runs of SSHAH3 at different elapsed times are given from simulation results. The times development of flows are shown in Fig.3, 4 and 5. These fields illustrate the different elapsed times that are used in the initial stage and the density flow reaches the dam. The simulation results give the contours of the velocity fields. Fig. 3 shows the initial velocity field is forward at all points.

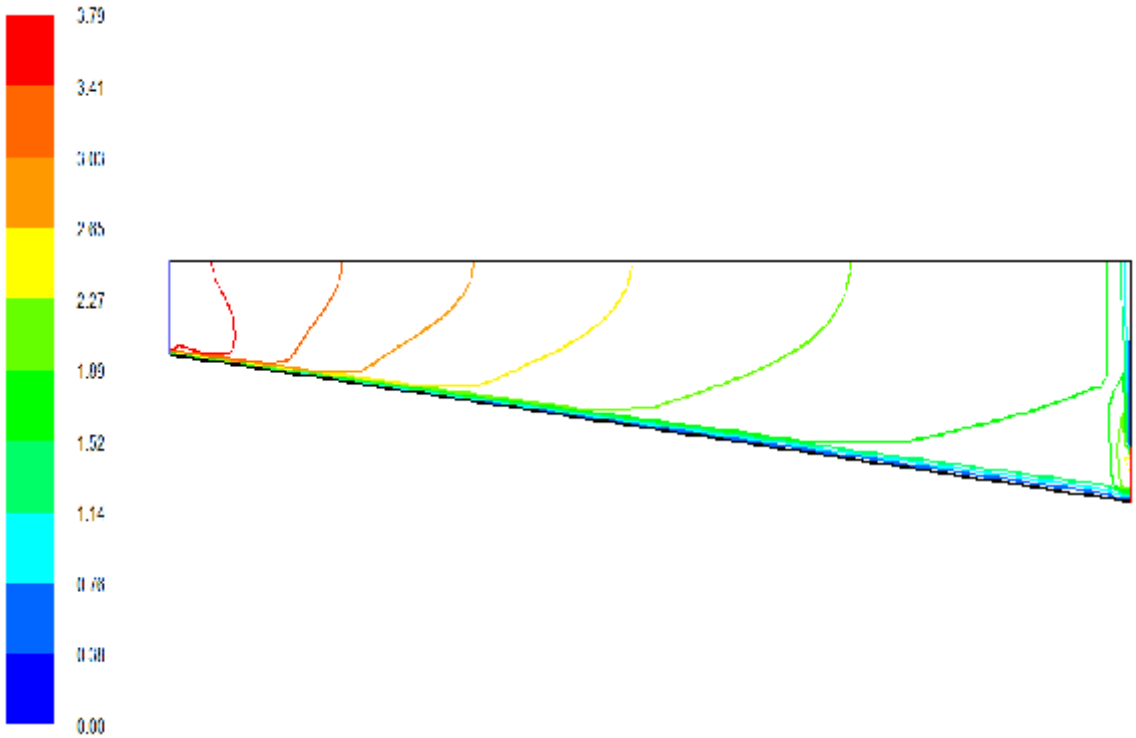

Figure 3. Initially typical velocity contour field, (elapsed time is 30 seconds)

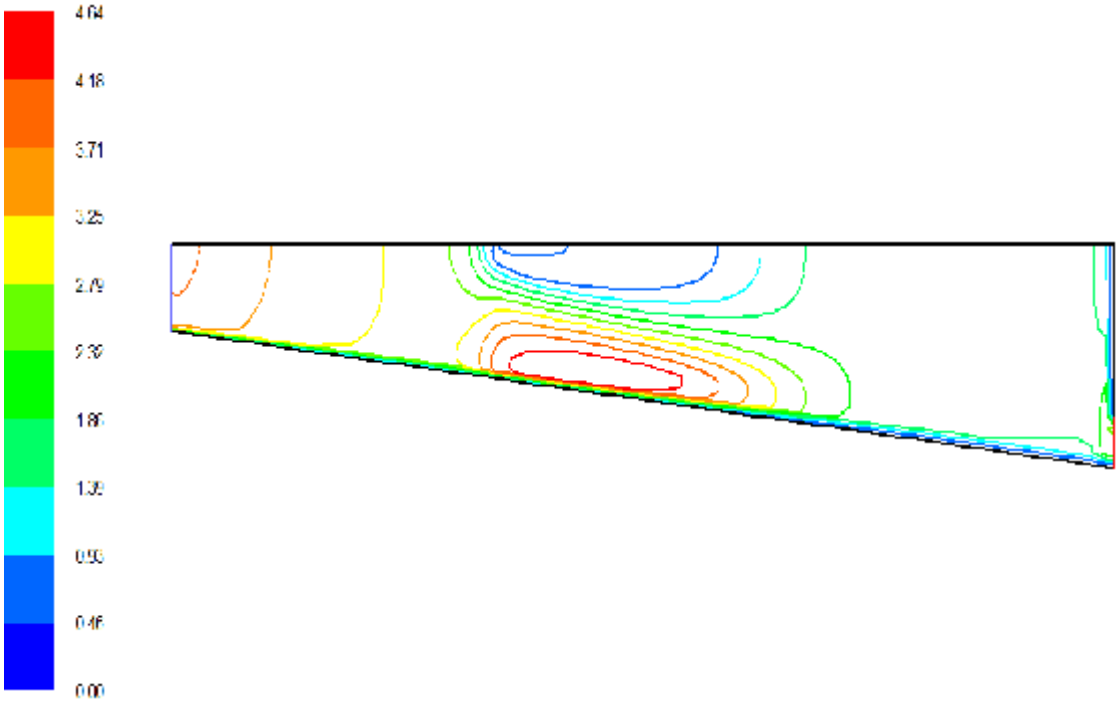

Figure 4. Reservoir velocity contour field at initiation of circulation flow for experimental SSHAH3 (elapsed time is 210 seconds).

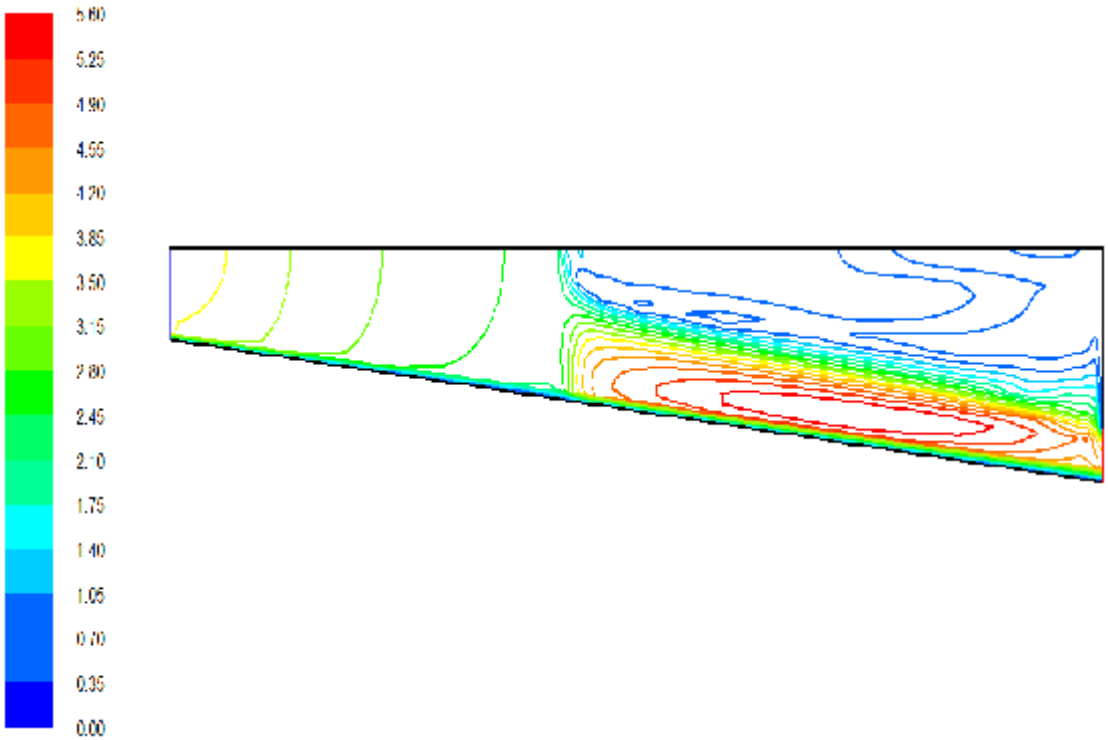

Figure 5. Reservoir velocity contours after density flow reached the dam for experimental SSHAH3 (elapsed time is 600 seconds).

Fig. 4 show velocity contour field for the elapsed time 210 seconds after plunging. The situation at this time is just the appearance of a small region of backflow over the plunging flow where the velocities are about 4.68 cm/s. Fig. 5 show that the density flow reached the dam face at the elapsed time of 600 seconds and at the same time recirculation region reached the dam too. The recirculation region grows and cover the entire reservoir and maximum velocities appear in the under flow region. The velocities in the Figure increase from 3.71 cm/s to 5.60 - 5.79 cm/s during the run elapsed time. This velocity increment is important for reservoir bottom stability. The reason for the velocity increment can be explained with increases bottom slope and with charging balance of force. This feature is appeared in all the other model simulations and experimental measurement.

Variation of vertical velocity profiles at the plunging point

Both experimental (for run SSHAH3) and numerical simulations of velocity profiles near the plunging point are given in Fig. 6. The comparison of these profiles shows an excellent agreement between the experimental and the present model simulations. The maximum percentage difference between the present model results and that of Singh and Shah is 11%.

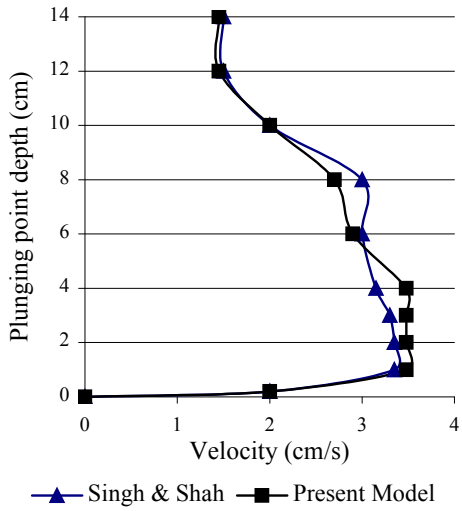

Figure 6. Comparison of experimental and numerical velocity profiles near the plunge point, for run SSHAH3.

CONCLUSION

A mathematical model was derived to investigate the characteristic parameters of the density and plunging flow in a dam reservoir. The model was solved numerically using FLUENT and analyzed to determine density flow characterizing parameters. The results followed such an expected trend based on the plunging flow dynamics.

Plunging flow, density flow and recirculation zone development were well defined in the velocity, temperature and turbulence fields from the model simulation figures. The results of this mathematical model were compared with the available experimental and mathematical model results. The comparison revealed an excellent agreement.

The present model simulations provide useful information for understanding and determining plunging flow patterns as well as density flow in a dam reservoir.

REFERENCES

[1] Ünes, F. (2008) Investigation of density flow in dam reservoirs using a three-dimensional mathematical model including Coriolis effect, Computers & Fluids , 37, 1170-1192.

[2] Ünes, F. (2008) Analysis of Plunging Phenomenon in Dam Reservoirs Using Three Dimensional Density Flow Simulations, Canadian Journal of Civil Engineering , 35, 1138-1151.

[3] Farrell, G.J., Stefan, H.G. (1986) Buoyancy induced plunging flow into reservoirs and coastal regions, Project Report, No. 241, St. Anthony Falls Hydr. Lab., University of Minnesota.

[4] Üneş, F. (2004) Investigation of effects of coriolis forces and outlet levels on reservoir flow using mathematical model, Istanbul Technical University, Ph.D. Dissertation, Institute of Science and Technology, İstanbul.

[5] Singh, B., Shah, C.R. (1971) Plunging phenomenon of density currents in reservoirs, La Houille Blanche, 26, 59-64.

[6] Akiyama, J., Stefan, G.H. (1984) Plunging Flow into a Reservoir, Theory, Journal of Hydraulic Engineering, ASCE, 110, 484-489.

[7] Farrell, G.J., Stefan, H.G. (1988) Mathematical Modeling of Plunging Reservoir Flows, Journal of Hydraulics Research**,** 26, 525-537.

[8] Johnson, T.R., Farrell, G.J., Ellis C.R., Stefan H.G.(1987) Negatively Buoyant Flow in Diverging Channel: Part I: Flow Regimes, Journal Hydraulic Engineering ASCE, 113, 716-730.

[9] Johnson, T.R., Ellis C.R., Stefan H.G.(1987) Negatively Buoyant Flow in Diverging Channel: Part II: 3-D Flow Field Regimes, Journal Hydraulic Engineering ASCE**,** 113, 731-742.

[10] Lee, H.Y., Yu, W.S. (1997) Experimental Study of Reservoir Turbidity Current, Journal Hydraulic Engineering, 123 (6), 520-528.

[11] Kassem, A., Imran, J., Khan, J.A. (2003) Three-Dimensional Modeling of Negatively Buoyant Flow in Diverging Channels, Journal Hydraulic Engineering , 129 (12), 936-947.

[12] Üneş, F., Ağıralioğlu, N. (2004) Investigation of density plunging reservoir flow using mathematical modeling, İTÜ Journal/d, 3 (6), 47-58.

[13] Launder, B.E., Spalding, D.B. (1972) Mathematical models of Turbulence, Academic Press, New York.

[14] Launder, B.E., Spalding, D.B. (1972) A Calculation Procedure for Heat, Mass and Momentum Transfer in Three Dimensional Parabolic Flows, International Journal Heat and Mass Transfer, 15, 1787-1806.

[15] Rodi, W. (1984) Turbulence Models and Their Application in Hydraulics: A State of the Art Review. IAHR, Delft, The Netherlands.

[16] FLUENT 6.3 users Guide, FLUENT incorporated, 2007.